environmental microbiology

Environmental Microbiology (2021) **23**(11), 6953–6964 doi:10.1111/1462-2920.15739

Physiology and genetics of ethanologenesis in the acetogenic bacterium *Acetobacterium woodii*

Jimyung Moon and Volker Müller *

Molecular Microbiology & Bioenergetics, Institute of Molecular Biosciences, Johann Wolfgang Goethe University, Max-von-Laue Str. 9, Frankfurt, D-60438, Germany.

Summary

The acetogenic model bacterium *Acetobacterium woodii* is well-known to produce acetate by homoacetogenesis from sugars, but under certain conditions minor amounts of ethanol are produced in addition. Here, we have aimed to identify physiological conditions that increase electron and carbon flow towards ethanol production. Ethanol was only produced from fructose but not from $H_2 + CO_2$, formate, pyruvate, lactate or alanine. In the absence of Na^+, the Wood–Ljungdahl pathway (WLP) of acetate formation is not functional. Therefore, the ethanol yield increased to 0.42 mol/mol (ethanol/fructose) with an ethanol/acetate ratio of 0.28 mol/mol. The presence of bicarbonate/CO_2 stimulated electron and carbon flow through the WLP and led to less ethanol produced. Of the 11 potential alcohol dehydrogenase genes, the most upregulated during ethanologenesis was *adh4*. A deletion of *adh4* led to an increase in ethanol production by 100% to a yield of 0.79 mol/mol (ethanol/fructose); this correlated with an increase in transcript abundance of *adh6*. In sum, our studies revealed low Na^+ and bicarbonate/CO_2 as factors that trigger ethanol formation and that a deletion of *adh4* drastically increased ethanol formation in *A. woodii*.

Introduction

Global reduction of CO_2 emissions while still providing energy for the society is currently one of the biggest challenges for mankind (Fawzy *et al*., 2020). However, not only reducing emissions but also reducing atmospheric CO_2 concentrations by carbon capture and storage (CCS) or carbon capture and utilization (CCU) is of utmost importance (Gabrielli *et al*., 2020). Biological solutions for CCS and CCU are available and steadily increasing (Daniell *et al*., 2012). Among the bacteria that can be used for CCU and CCS are the anaerobic, acetate-forming (acetogenic) bacteria that grow in the dark lithotrophically or organotrophically. Lithotrophically they produce acetate from $H_2 + CO_2$ or CO or a combination thereof (synthesis gas) by a special pathway, the Wood–Ljungdahl pathway (WLP) (Wood and Ljungdahl, 1991; Müller, 2019). The WLP is an ancient pathway of CO_2 fixation and in these bacteria coupled to the net synthesis of ATP, whereas all other pathways for CO_2 fixation require the net input of cellular energy, ATP (Poehlein *et al*., 2012; Schuchmann and Müller, 2014). Acetate is the only or major product in most species but some acetogenic bacteria can produce ethanol naturally, albeit in minor amounts. The industrial production of bioethanol from syngas using the acetogen *Clostridium autoethanogenum* has already been implemented (Liew *et al*., 2016a; Liew *et al*., 2016b; Liew *et al*., 2017).

Ethanol formation from CO_2 via the WLP in acetogens could go two ways. One is via acetyl-CoA to acetaldehyde and then ethanol, catalysed by aldehyde and ethanol dehydrogenases (Dien *et al*., 2003). This pathway is thermodynamically restricted. Activation of CO_2 via formate to formyl-tetrahydrofolate, the first steps in the WLP, requires the hydrolysis of ATP (Ljungdahl, 1986). This ATP is regained by conversion of acetyl-CoA to acetyl-phosphate, followed by substrate-level phosphorylation during acetate formation from acetyl-phosphate (Müller, 2003). This ATP is missing when acetyl-CoA is reduced to ethanol and therefore, ethanol can, if at all, only be a minor end product alongside acetate. Unless the bacteria have a special enzyme, like *C. autoethanogenum* or *Clostridium ljungdahlii*, an aldehyde:ferredoxin oxidoreductase (AOR) that activates the acetate produced to acetaldehyde at the expense of oxidation of the strong reductant, reduced ferredoxin (White *et al*., 1993; Richter *et al*., 2016b; Liew *et al*., 2017). Thereby, ethanol and ATP are produced.

Unfortunately, one of the best-studied acetogens to date, *Acetobacterium woodii* lacks an *aor* gene (Poehlein *et al*., 2012) and, therefore, ethanol formation

Received 7 July, 2021; accepted 22 August, 2021. *For correspondence. E-mail vmueller@bio.uni-frankfurt.de; Tel. 49-69-79829507; Fax 49-69-79829306.

from $H_2 + CO_2$ has never been observed. In contrast, *A. woodii* has been shown to produce ethanol from sugar already in 1989 (Buschhorn *et al*., 1989) but the conditions required for the cells to produce ethanol have not been analysed in detail. Phosphate limitation was unravelled to be of vital importance for ethanol formation and a sugar concentration of 40 mM but not 20 mM triggered ethanol formation at 120 mM bicarbonate in the medium (Buschhorn *et al*., 1989). Knowledge of the genes/proteins involved in ethanol formation and conditions that trigger ethanol formation would be a prerequisite to metabolically engineer *A. woodii* to produce ethanol from $H_2 + CO_2$. We have followed up these observations and studied and optimized ethanol production from fructose by *A. woodii*.

Results

Ethanol production by A. woodii *during growth on fructose*

To study ethanol production in *A. woodii*, we first checked the growth substrate dependence of ethanol formation. Therefore, growth experiments were performed with different carbon and energy sources. Ethanol formation was not observed during growth on $H_2 + CO_2$, formate, pyruvate, lactate, or alanine. It had been reported that *A. woodii* produced ethanol at 40 but not 20 mM glucose under phosphate limitation (2.2 mM); under these conditions, cells produced 14 mM ethanol from 40 mM glucose with an ethanol yield ($Y_{ethanol/hexose}$) of 0.35 (mol/mol; ethanol/glucose) (Buschhorn *et al*., 1989). To unravel factors triggering ethanol formation, we determined growth and ethanol yields under eight different conditions (Fig. 1A). First, *A. woodii* grown on 60 mM fructose showed improved ethanol yields compared to the cells grown on 20 mM fructose, confirming the hypothesis that a high carbon/electron load shifts the carbon flow (Buschhorn *et al*., 1989). During growth on 20 mM fructose, ethanol was not formed. Buschhorn *et al*. (1989) used 120 mM bicarbonate in their media but did not report on the effect of the bicarbonate concentration on ethanol formation. Here, cells grown on 60 mM fructose in the presence of 60 mM $KHCO_3$ produced only 0.8 $\pm$ 0.1 mM ethanol, but 6 $\pm$ 1 mM ethanol was produced by cells grown in the presence of 120 mM $KHCO_3$ with an ethanol yield of 0.14 $\pm$ 0.03 mol/mol. The WLP in *A. woodii* requires Na^+ for activity (Heise *et al*., 1989; Müller *et al*., 1990; Westphal *et al*., 2018). Interestingly, removal of NaCl from the medium (the residual Na^+ concentration was 100 μM) strongly increased ethanol production with a highest ethanol yield of 0.42 $\pm$ 0.05 mol/mol with 60 mM of fructose, which corresponds to 21 $\pm$ 2% electrons used for ethanol formation. It is important to note that in the absence of NaCl, ethanol formation was no longer stimulated by bicarbonate.

For further analyses, *A. woodii* was grown on 60 mM fructose under Na^+ depletion and growth and products were monitored over time (Fig. 1B). Cells grown on 60 mM fructose under Na^+ depletion reached a maximum optical density (OD_{600}) of 3 with a growth rate of 0.15 $\pm$ 0.01 h^{-1} and a doubling time of 4.6 $\pm$ 0.2 h, which was 25% slower than under Na^+-rich condition (20 mM NaCl) (Fig. 1C). Ethanol was not found in the exponential growth phase, but it started being formed after reaching the stationary phase, at around 40 h. During 210 h of incubation, 37 $\pm$ 1 mM fructose was utilized, and 16 $\pm$ 2 mM ethanol and 57 $\pm$ 2 mM acetate were produced with an ethanol/acetate ratio of 0.28 $\pm$ 0.03 mol/mol. On the contrary, under Na^+-rich conditions, 86 $\pm$ 2 mM acetate and only 0.8 $\pm$ 0.1 mM ethanol was formed from 35 $\pm$ 1 mM fructose (Fig. 1C). In the exponential growth phase, the pH of the medium decreased drastically due to acetate formation and the pH value at which ethanol formation started was around 6.5. This phenomenon, that ethanol production is triggered by low pH (solventogenesis) has been also observed in other ethanol-producing acetogens such as *C. ljungdahlii* (Richter *et al*., 2016a; Richter *et al*., 2016b). As minor products, we observed 1 mM lactate and 2 mM alanine but no H_2 or formate.

Ethanol production is stimulated in the absence of Na^+

Maximal ethanol formation in growing cells was observed in media depleted of Na^+. The effect of Na^+ on ethanol formation from fructose was further investigated in resting cells of *A. woodii*, in which metabolism is uncoupled from growth. For these experiments, cells were grown on 60 mM fructose in the presence or absence of 20 mM NaCl until stationary growth phase and after harvesting the cells, the cell suspensions were prepared as described in Experimental procedures. First, ethanol production was monitored in cell suspensions prepared from cells grown under Na^+-depleted conditions. The cells were resuspended in cell suspension buffer supplemented either with 20 mM or without NaCl. In Na^+-depleted buffer, the cells utilized 34 $\pm$ 1 mM fructose and produced 14 $\pm$ 1 mM ethanol and 63 $\pm$ 1 mM acetate with an ethanol yield of 0.41 $\pm$ 0.02 mol/mol and an ethanol/acetate ratio of 0.22 $\pm$ 0.01 (Fig. 2A). Acetate was rapidly formed in the first 4 h with a rate of 63 $\pm$ 4 nmol min^{-1} mg^{-1}. After 9 h of incubation, when the pH of the buffer decreased from 7.6 to 6.7, ethanol formation started and proceeded with a rate of 7 $\pm$ 1 nmol min^{-1} mg^{-1}, a rate comparable to ethanol formation by growing cells. The final pH value of the buffer was 5.2. When 20 mM NaCl was added to the cell

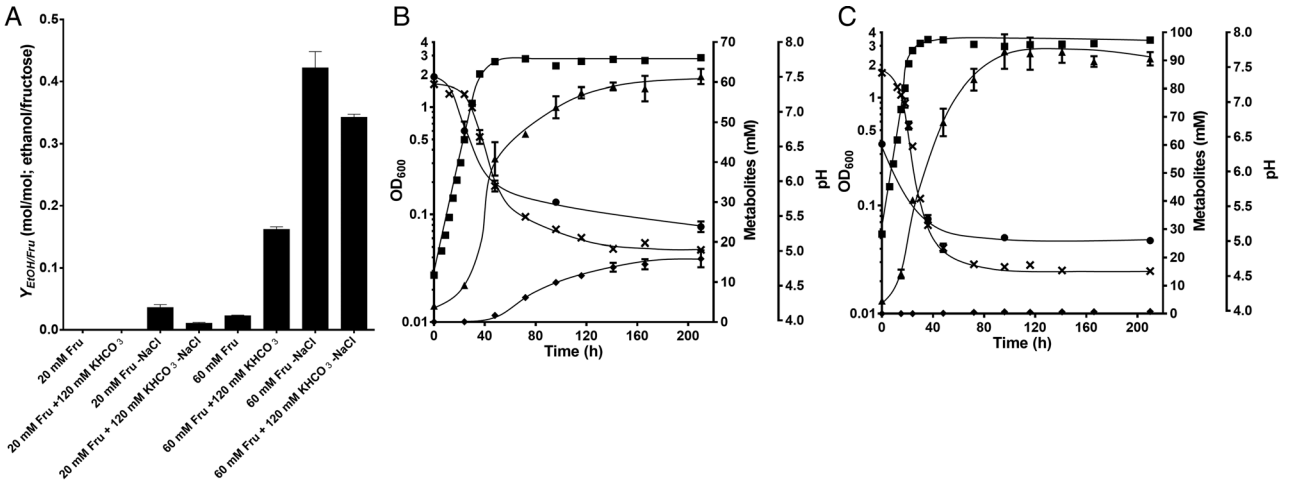

Fig. 1. Ethanol formation in growing cells of *A. woodii* during fructose fermentation.
A. Growth experiments were carried out in 50 ml media in 115 ml serum flasks at 30°C with 20 or 60 mM fructose. Depicted are the ethanol yields determined after 90 h (20 mM) or 210 h (60 mM) of incubation. Each column indicates a mean with standard error of the mean (SEM); $n = 3$ independent experiments. Growth and ethanol production of *A. woodii* on 60 mM fructose in (B) Na^+-depleted complex medium or (C) Na^+-rich complex medium. Optical densities (■), pH (×), fructose (●), acetate (▲) and ethanol (♦) were determined. Except OD (representative), each data point indicates a mean with SEM; $n = 3$ independent experiments.

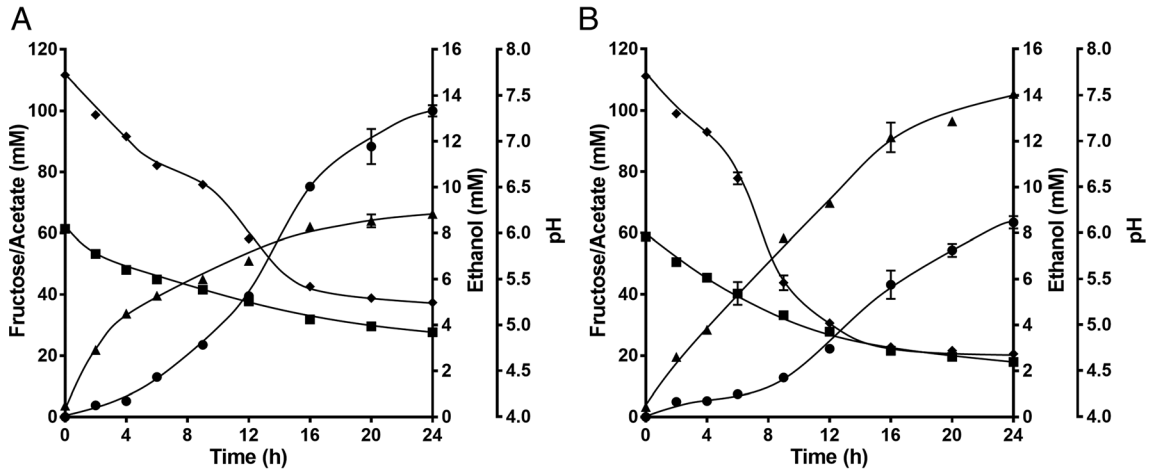

Fig. 2. Ethanol formation in resting cells of *A. woodii* grown under Na^+-depleted conditions. Cells were grown in Na^+-depleted media with 60 mM fructose and harvested in the early stationary growth phase. After washing twice, the cells were resuspended in 20 ml of Na^+-depleted (A) or 20 mM NaCl-containing (B) cell suspension buffer in 115 ml serum flasks under an N_2/CO_2 atmosphere at a total protein concentration of 2 mg ml^{-1}. 60 mM of fructose was given to the cell suspensions as carbon source. Fructose (■), acetate (▲), ethanol (●) and pH (♦) were determined at each time point. Each data point indicates a mean ± SEM; $n = 3$ independent experiments.

suspensions (Fig. 2B), fructose consumption increased to 41 mM, however, only 9 ± 0 mM ethanol was produced with a formation rate of 4 ± 0 nmol min^{-1} mg^{-1} (57% of that in Na^+-depleted buffer) despite the low pH of the buffer. Instead, acetate formation increased with a final concentration of 102 ± 2 mM and this caused a lower final pH of 4.7. The ethanol yield and the ethanol/acetate ratio decreased to 0.20 ± 0.01 mol/mol and 0.08 ± 0.01 mol/mol, respectively, which are less than 50% of that in Na^+-depleted buffer.

The same cell suspension experiments were performed with cells grown under Na^+-rich conditions. Overall, ethanol production by these cells was much smaller compared to those prepared from cells grown under Na^+-depleted conditions, regardless of the presence of 20 mM NaCl in buffer. This implies that the presence/absence of Na^+ not only causes metabolic shifts but is also involved in regulatory circuits affecting genes/proteins involved in ethanol formation. Cells suspended in Na^+-rich buffer (Fig. 3A) fermented 38 ± 0 mM

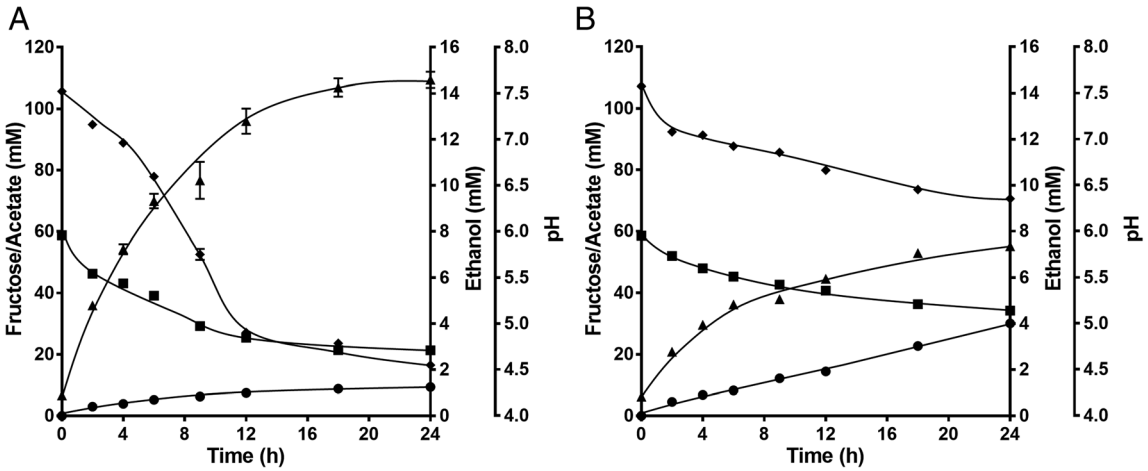

Fig. 3. Ethanol formation in resting cells of *A. woodii* grown under Na^+-rich conditions. Cells were grown in Na^+-rich (20 mM) media with 60 mM fructose and harvested in the early stationary growth phase. After washing twice, the cells were resuspended in 20 ml of 20 mM NaCl-containing (A) or Na^+-depleted (B) cell suspension buffer in 115 ml serum flasks under an N_2/CO_2 atmosphere at a total protein concentration of 2 mg ml^{-1}. 60 mM of fructose was given to the cell suspensions as carbon source. Fructose (■), acetate (▲), ethanol (●) and pH (♦) were determined at each time point. Each data point indicates a mean ± SEM; $n = 3$ independent experiments.

fructose to 103 ± 5 mM of acetate but only 1 ± 0 mM of ethanol. Removal of NaCl from the buffer (Fig. 3B) triggered ethanol production even if the resting cells were from cells cultivated under Na^+-rich conditions. As the cells were not adapted to Na^+-depleted conditions, the fructose consumption decreased to 24 ± 0 mM, however, four times more ethanol was formed compared to the cell suspensions in Na^+-rich buffer, with an ethanol yield of 0.16 ± 0.01 mol/mol.

Ethanol formation is stimulated at low pH

In growing as well as resting cells, ethanol production under Na^+-depleted conditions started when the pH of the media/buffer decreased to pH 6.5–6.7. This implies that a low pH favours ethanol over acetate formation. To test the effect of the initial pH on ethanol formation, cell suspensions were prepared in imidazole buffer with initial pH values of 6.2, 6.6 and 6.9. Indeed, a low initial pH of the buffer improved the ethanol yield (Fig. 4). While the cell suspensions with an initial pH value of 7.4 reached a yield of 0.42 ± 0.00 mol/mol, the ethanol yield from those with an acidic pH increased to 0.46 ± 0.00 mol/mol at pH 6.9, 0.54 ± 0.00 mol/mol at pH 6.6, and 0.60 ± 0.03 mol/mol at pH 6.2, respectively. In the cell suspensions with an initial pH of 6.2, ethanol was immediately produced at early stage of incubation with a three times higher production rate (6.5 ± 0.2 nmol min^{-1} mg^{-1}) compared to pH 7.4 (2.2 ± 0.2 nmol min^{-1} mg^{-1}), even though fructose consumption and acetate formation decelerated to 60% at pH 6.2 (Fig. S1). With an initial pH of 6.2, the cell suspensions produced 9 ± 1 mM ethanol and 27 ± 0 mM acetate from 15 ± 0 mM fructose with an

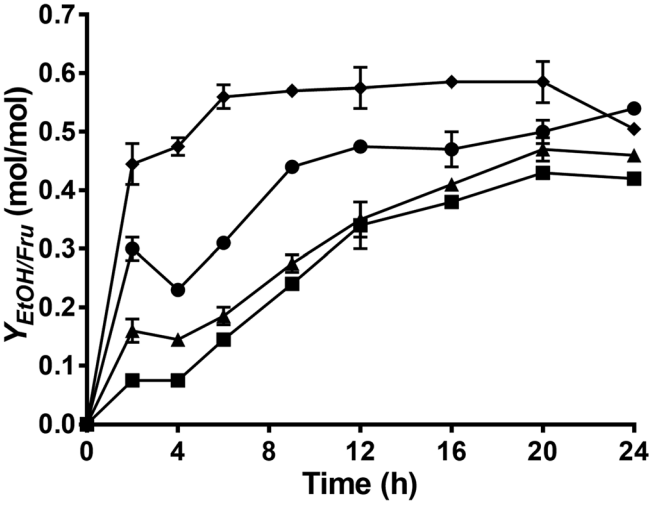

Fig. 4. A low initial pH increases ethanol yields in resting cells of *A. woodii*. Cells were grown in Na^+-depleted media with 60 mM fructose and harvested in the early stationary growth phase. After washing twice, the cells were resuspended in 20 ml of Na^+-depleted cell suspension buffer with an initial pH of 7.4 (■), 6.9 (▲), 6.6 (●), or 6.2 (♦) in 115 ml serum flasks under an N_2/CO_2 atmosphere at a total protein concentration of 2 mg ml^{-1}. 60 mM of fructose was given to the cell suspensions as carbon source. Each data point indicates a mean ± SEM; $n = 2$ independent experiments.

ethanol/acetate ratio of 0.34 ± 0.03 mol/mol. Even if the final ethanol concentration was higher with an initial pH of 7.4 (17 ± 0 mM ethanol out of 41 ± 0 mM fructose), this result showed that a low initial pH of the buffer shifted carbon flow towards ethanol synthesis. The same experiments were carried out in buffers with a high initial pH of 8.0, 8.5, or 9.0, however, ethanol yields decreased to 47% (at pH 8.0 and 8.5, 0.20 mol/mol; at pH 9.0, 0.19 mol/mol) compared to that of the resting cells at pH 7.4.

Effect of bicarbonate/CO_2 on ethanol formation in the cell suspensions

The effect of bicarbonate/CO_2 on ethanol formation in growing cells of *A. woodii* was unclear. High concentrations of bicarbonate (120 mM) increased ethanol production under Na^+-rich conditions but reduced the ethanol yield under Na^+-depleted conditions. To analyse the effect of bicarbonate on metabolism only, experiments with non-growing, resting cells were performed. Cells were grown in Na^+-depleted media and the cell suspension experiments were carried out with buffers supplemented with 0, 60, 120, or 180 mM $KHCO_3$. Under Na^+-depleted conditions, high concentrations of $KHCO_3$ in the buffer hindered ethanol formation, even though more fructose was consumed (Fig. 5A). The cell suspensions in buffer with 120 mM $KHCO_3$ produced only 12 $\pm$ 2 mM ethanol from 44 $\pm$ 2 mM fructose with a reduced ethanol yield of 0.26 $\pm$ 0.03 mol/mol. Cells incubated in buffer with 180 mM $KHCO_3$ formed only 3 $\pm$ 0 mM ethanol from 53 $\pm$ 0 mM fructose, reaching a yield of 0.08 $\pm$ 0.01 mol/mol. In contrast, removal of $KHCO_3$ increased ethanol production to a yield of 0.58 $\pm$ 0.02 mol/mol. 14 $\pm$ 0 mM ethanol was produced from 24 $\pm$ 0 mM fructose with a four times faster initial formation rate (8.1 $\pm$ 0.3 nmol min^{-1} mg^{-1}) compared to those in buffer with 60 mM $KHCO_3$ (2.2 $\pm$ 0.2 nmol min^{-1} mg^{-1}). The ratio of ethanol/acetate increased to 0.32 $\pm$ 0.04 mol/mol. Interestingly, the same phenomenon was observed under Na^+-rich conditions, which is contradictory to the observation in growing cells. While the increase of $KHCO_3$ from 60 to 120 mM in growing cells improved the ethanol yield from 0.02 to 0.14 mol/mol, the yield in cell suspensions decreased with increasing $KHCO_3$ concentrations (Fig. 5B). Instead, the removal of $KHCO_3$ stimulated ethanol production even under Na^+-rich conditions. Cell suspensions in HCO_3^--depleted buffer produced 5 $\pm$ 0 mM ethanol from 24 $\pm$ 0 mM fructose with a yield of 0.19 $\pm$ 0.00 mol/mol, which is four times higher than that of the cell suspensions incubated in the presence of 60 mM $KHCO_3$. In sum, removal of $KHCO_3$ stimulated ethanol formation in resting cells of *A. woodii* under both Na^+-depleted and Na^+-rich conditions.

Expression analysis of potential alcohol dehydrogenase genes in A. woodii *via semiquantitative PCR*

Independent of the way used for ethanol formation, the last enzyme involved is an alcohol dehydrogenase. The genome of *A. woodii* has 11 genes annotated as putative Adhs; seven for alcohol dehydrogenases (*adh1-7*), one for a bifunctional aldehyde/alcohol dehydrogenase (*adhE*), two for butanol dehydrogenases (*bdh1*, *bdh2*) and one for a 1,3-propanediol dehydrogenase (*dhaT*) (Poehlein *et al*., 2012). So far, only AdhE and Adh4 have been studied. AdhE is a bifunctional CoA-dependent aldehyde and alcohol dehydrogenase which is responsible for the initial oxidation of ethanol to acetyl-CoA during growth on ethanol (Bertsch *et al*., 2016). Adh4 catalyses the reduction of propionaldehyde to propanol during 1,2-propanediol metabolism within the bacterial microcompartments (BMC) (Chowdhury *et al*., 2021). To possibly identify the genes involved in the observed ethanol

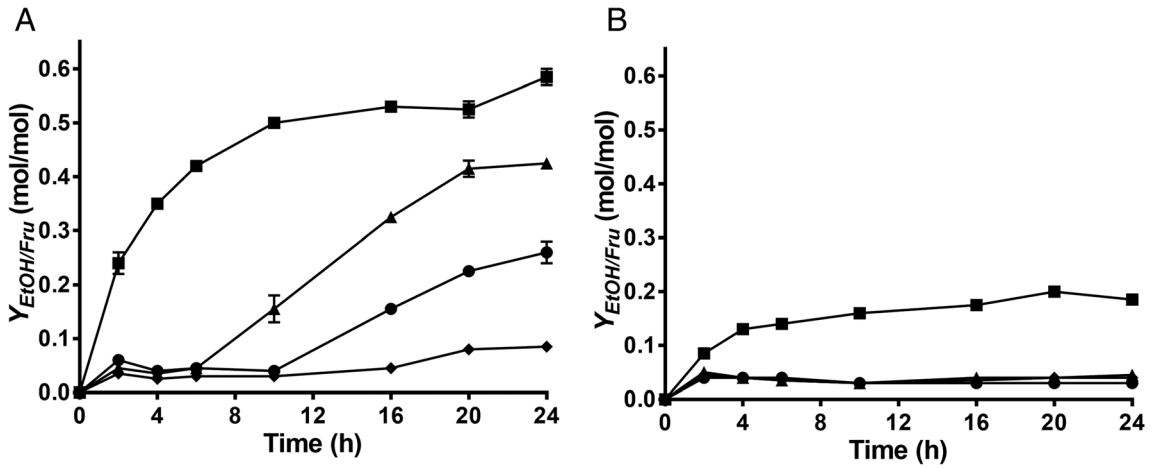

Fig. 5. Bicarbonate dependence of ethanol formation in resting cells of *A. woodii* under Na^+-depleted (A) and Na^+-rich (B) conditions. Cells were grown in Na^+-depleted (A) or Na^+-rich (B) media with 60 mM fructose and harvested in the early stationary growth phase. After washing twice, the cells were resuspended in 20 ml of Na^+-depleted (A) or 20 mM NaCl-containing (B) cell suspension buffer either without $KHCO_3$ (■) under an N_2 atmosphere or with 60 (▲), 120 (●), or 180 mM $KHCO_3$ (♦) under an N_2/CO_2 atmosphere at a total protein concentration of 2 mg ml^{-1}. 60 mM of fructose was given to the cell suspensions as carbon source. Each data point indicates a mean $\pm$ SEM; $n = 2$ independent experiments.

formation, cells were grown under conditions that allow for ethanol formation and conditions that do not, RNA was isolated and the transcript levels of putative *adh* genes was monitored with semiquantitative polymerase chain reaction (PCR). For this, mRNA was prepared from cells grown on either 20 or 60 mM fructose under Na^+-rich or Na^+-depleted conditions and harvested either in the exponential (OD_{600} of 0.5) or stationary (OD_{600} of 1.8) growth phase, and cDNA was synthesized as described in Experimental procedures. First, the quality of cDNA was tested by comparing a housekeeping gene *gyrA* (DNA gyrase subunit A; Awo_c00060) and a highly expressed gene, *pduT* (BMC shell protein; Awo_c25740) and the transcript abundance of both genes were similar in all conditions (Fig. S2). No significant transcript levels were found for *adh1* (Awo_c04150), *adh5* (Awo_c14890) and *dhaT* (Awo_c17360). As already shown by Bertsch *et al*. (2016), the *adhE* gene (Awo_c06310) was not expressed during fructose fermentation. *adh2* (Awo_c05670; located in the diguanylate cyclase operon) transcript was found in cells grown on 60 mM fructose with NaCl and harvested in the stationary growth phase as well as in cells cultivated under Na^+-depleted conditions. The *adh3* gene (Awo_c06180) was upregulated in ethanol-forming cells grown on 60 mM fructose under Na^+-depletion. The gene encoding Adh4 (Awo_c06220), which is responsible for propanol formation during 1,2-propanediol metabolism and that has also high specific activity of acetaldehyde reduction (Chowdhury *et al*., 2021), was expressed significantly at stationary growth phase regardless of fructose concentration and presence of NaCl. The *adh6* (Awo_c26370) and *adh7* gene (Awo_c25140; annotated as pyridoxin kinase) were similarly expressed under all conditions. Same was observed for the genes *bdh1* (Awo_c00730) and *bdh2* (Awo_c02950) (Fig. S2). We further determined the upregulation of *adh3*, *adh4* and *adh6* genes under ethanol-forming condition using real-time quantitative PCR (qPCR). Compared to the non-ethanol forming conditions (20 mM fructose under Na^+-rich conditions), the *adh3* gene was upregulated 2.1 $\pm$ 0.8 fold (log_2 fold change of 1.0) at the exponential growth phase and 2.7 $\pm$ 0.2 fold (log_2 fold change of 1.4) at the stationary growth phase under ethanol-forming conditions (60 mM fructose under Na^+-depleted conditions) (Fig. 6). However, the *adh4* gene showed higher expression levels with a fold change of 4.2 $\pm$ 1.8 (log_2 fold change of 2.0) at the exponential growth phase and 8.3 $\pm$ 1.0 (log_2 fold change of 3.0) at the stationary growth phase. As also shown in semi-qPCR results, the *adh6* gene was similarly expressed with a fold change of 1.1 $\pm$ 0.1 (log_2 fold change of 0.1) at the exponential growth phase and 1.5 $\pm$ 0.1 (log_2 fold change of 0.6) at the stationary growth phase.

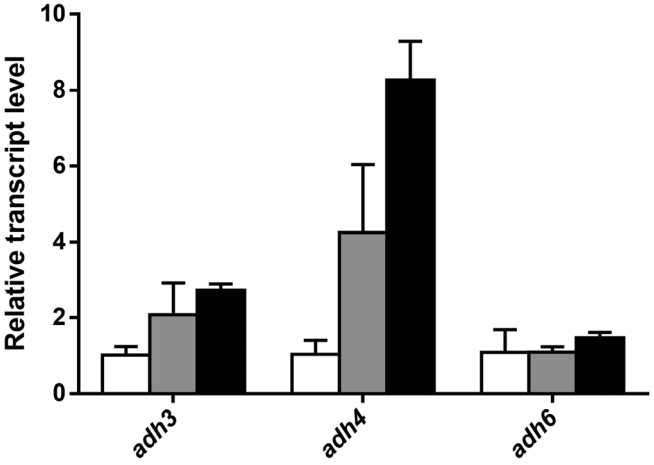

Fig. 6. Quantification of transcript levels of *adh3*, *adh4* and *adh6* in *A*. *woodii* under ethanol forming condition. cDNA was synthesized from the cells grown in Na^+-depleted complex media with 60 mM fructose and harvested either at exponential (grey bars) or stationary growth phase (black bars). The transcript levels of *adh3*, *adh4* and *adh6* genes were analysed with quantitative real-time PCR and the relative expression was normalized to a housekeeping gene *gyrA*. As control, cDNA of *A*. *woodii* grown on 20 mM fructose under Na^+-rich conditions and harvested at exponential growth phase (non-ethanol forming) was used (white bars). Each data point indicates a mean $\pm$ SEM; $n = 4$ independent experiments.

Mutational analysis of selected adh *genes*

In order to identify the ethanol forming alcohol dehydrogenase, we deleted the *adh3* gene which was upregulated to some extent under ethanol forming conditions. In addition, *adh6* (unknown function, not differentially regulated, upregulated during growth on propanediol) (Chowdhury *et al*., 2021) should be deleted. The Δ*adh4* mutant previously described (Chowdhury *et al*., 2021) should be also analysed due to the higher gene expression levels under ethanol forming conditions. To this end, suicide plasmids pMTL84151_JM_dadh3 and pMTL84151_JM_dadh6 were constructed, which carry each 1000 bp of upstream and downstream flanking regions (UFR and DFR) of the *adh3* or *adh6* gene leaving 3 bp behind the start codon and 3 bp in front of stop codon. For selection, the plasmids contained the *pyrE* gene from *Clostridium acetobutylicum* (Westphal *et al*., 2018) and the chloramphenicol/thiamphenicol resistance cassette (*catP*) from *Clostridium perfringens* (Werner *et al*., 1977). First, the plasmids were integrated into the chromosome of *A*. *woodii* Δ*pyrE* at one flanking region under antibiotic pressure with thiamphenicol and subsequently, disintegration was forced by counter-selection with 5-fluoroorotate. The mutants were verified using PCR (Fig. S3).

Growth of the Δ*adh3* mutant under ethanol-forming conditions (60 mM fructose, -Na^+) was similar to the Δ*pyrE* mutant with a growth rate of 0.13 $\pm$ 0.00 h^{-1}

(Fig. 7A). The Δ*adh4* mutant had a slightly reduced growth rate (0.10 ± 0.00 h^{-1}). In contrast, growth of the Δ*adh6* mutant was much slower (0.05 ± 0.00 h^{-1}). The Δ*pyrE* mutant produced 12 ± 1 mM ethanol from 31 ± 0 mM fructose with an ethanol yield of 0.38 ± 0.02 mol/mol (Fig. 7B and C). The Δ*adh3* mutant produced the same amount of ethanol with the same ethanol yield. In the Δ*adh6* mutant, the rate of ethanol formation was slightly decreased, but the ethanol yield was the same as in the Δ*adh3* and Δ*pyrE* mutant. In sharp contrast, although the Δ*adh4* mutant consumed the same amount of fructose, it produced 100% more ethanol (25 ± 1 mM) than the Δ*pyrE* mutant with an ethanol yield of 0.79 ± 0.02 mol/mol; the ratio of ethanol/acetate was increased from 0.26 ± 0.01 to 0.63 ± 0.00 mol/mol. To see whether increased ethanol formation in Δ*adh4* correlated with a differential expression of the other alcohol dehydrogenase genes, their expression was analysed by semiquantitative PCR, as described above. Indeed, the transcript level of one gene, *adh6*, was drastically increased (Fig. 8). qPCR showed that *adh6* was upregulated 77 ± 11 fold (log_2 fold change of 6.3 ± 0.2) in the Δ*adh4* mutant.

Discussion

During sugar fermentation, ethanol can be synthesized in three different ways depending on how acetaldehyde is synthesized (Müller, 2014). First, pyruvate generated by glycolysis is directly converted to acetaldehyde and 2 CO_2 via pyruvate decarboxylase (Pdc) (Boiteux and Hess, 1970). Second, pyruvate is converted to acetate via pyruvate:ferredoxin oxidoreductase (PFOR), phosphotransacetylase (Pta) and acetate kinase (Ack), and the generated acetate is reduced to acetaldehyde via AOR using the strong reductant, ferredoxin to drive this

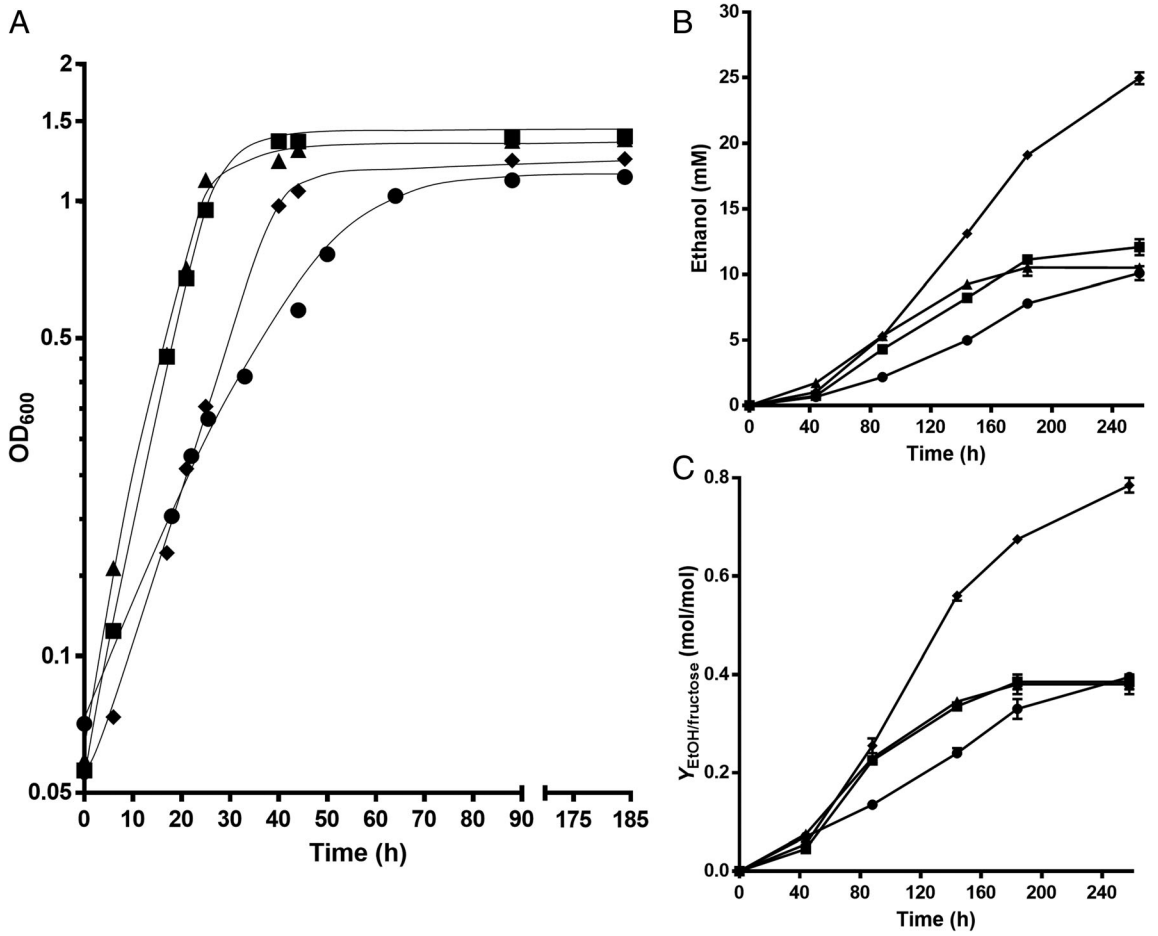

Fig. 7. Ethanol production in Δ*adh* mutants of *A. woodii* in Na^+-depleted media.
A. The Δ*adh3* (▲), Δ*adh4* (♦) and Δ*adh6* (●) mutants were grown in Na^+-depleted complex media with 60 mM fructose as carbon and energy source. The Δ*pyrE* mutant (■) was used as control. The growth experiments were performed in biological duplicates and one representative growth curve is presented. During growth, (B) ethanol formation and (C) ethanol yields were determined. Each data point indicates a mean ± SEM; $n = 2$ independent experiments.

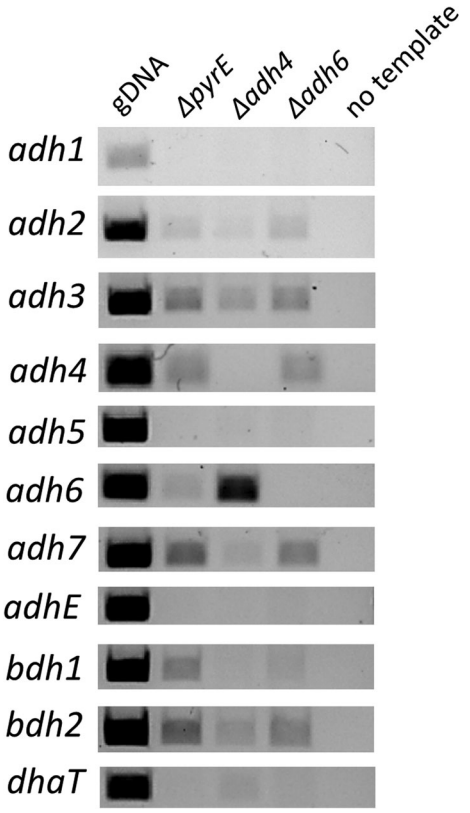

Fig. 8. Transcript abundance of the putative *adh* genes in *A. woodii* Δ*adh4* and Δ*adh6* mutants during fructose fermentation. Cells of the Δ*adh4*, Δ*adh6* and Δ*pyrE* mutant were grown on 60 mM fructose in the absence of NaCl. At the stationary growth phase, cells were harvested for mRNA preparation and cDNA synthesis. The transcript levels were analysed as presented in Fig. S2. Chromosomal DNA (gDNA) of *A. woodii* was used as positive control. No template was used for the last lane as negative control. The data shown are representative of two independent experiments.

reaction (Basen *et al*., 2014; Nissen and Basen, 2019). Lastly, acetaldehyde is synthesized from acetyl-CoA generated from glycolysis or WLP via a CoA-dependent aldehyde dehydrogenase (Aldh) in concert with an alcohol dehydrogenase or by a bifunctional alcohol dehydrogenase, AdhE (Membrillo-Hernandez and Lin, 1999; Bertsch and Müller, 2015; Liew *et al*., 2017). The genome of *A. woodii* does not contain genes encoding Pdc or AOR, but only genes encoding Aldh, Adh or AdhE (Poehlein *et al*., 2012). Therefore, ethanol can be only synthesized directly via acetyl-CoA reduction with a series of reactions catalysed by Aldh/Adh or by AdhE. A CoA-dependent acetaldehyde dehydrogenase has been purified from *A. woodii* (Buschhorn *et al*., 1992); the enzyme catalysed acetaldehyde oxidation with a specific activity of 4.5 U mg^{-1}, ethanol was not oxidized. The enzyme had two subunits of 40 and 28 kDa whose N-terminal amino acid sequence was determined (Buschhorn, 1989). With the now-known genomic sequence, it is now possible to find the encoding genes. Unfortunately, the proteins purified (or sequenced) by Buschhorn *et al*. (1992) are not an aldehyde dehydrogenase but formyl-THF synthetase (40 kDa) and alanine dehydrogenase (28 kDa). Moreover, the genome of *A. woodii* does not encode a two-subunit acetaldehyde dehydrogenase. The only potential acetaldehyde dehydrogenase genes in *A. woodii* are *pduP* (Awo_c25770) which is part of the 1,2-propanediol oxidation pathway (Schuchmann *et al*., 2015) and *aldH* (Awo_c33720).

In our expression analyses, the *adh3* gene was upregulated 2.7-fold under ethanol-forming conditions. The *adh3* gene localizes next to genes encoding a Sel1 repeat family protein (Awo_c06190) and PFOR (*porB*, Awo_c06200; *porA*, awo_c06210) in the same direction. The deduced protein Adh3 has a size of 45 kDa and is 68% similar to alcohol dehydrogenase of *Eubacterium limosum* (B2M23_15170) and *Eubacterium callanderi* (ELI_1601), and 45% similar to alcohol dehydrogenase of *C. acetobutylicum* (CA_P0059). It also has 39% similarity to L-threonine dehydrogenase YiaY of *Escherichia coli*. Unfortunately, deletion of *adh3* had no effect on ethanol formation. The *adh6* gene (Awo_c25140) was similarly expressed with a fold change of 1.5. This gene is located between two genes potentially encoding MFS_1 (major facilitator family) sugar transporter (Awo_c25400 and Awo_c25420). Adh6 has a size of 41 kDa and is 67% similar to lactaldehyde reductase of *Geosporobacter ferrireducens*. The heterogeneously produced protein did not catalyse acetaldehyde reduction. Again, deletion of *adh6* had no effect on ethanol formation.

Adh4, which is responsible for propanol formation during 1,2-propanediol metabolism, has also high specific activity for acetaldehyde reduction (Chowdhury *et al*., 2021); the *adh4* gene (Awo_c06220) was expressed significantly at the stationary growth phase regardless of the fructose concentration and presence or absence of NaCl. Interestingly, the transcript abundance of *adh4* was significant not only at the stationary growth phase (fold change 8.3) but also at the exponential growth phase (fold change 4.2) when cells were grown on 60 mM fructose under Na^{+}-depleted conditions. As described previously by Chowdhury *et al*. (2021), the *adh4* gene localizes as a single gene with a downstream gene encoding a potential LysR family transcriptional regulator (Awo _c06230). Adh4 has a size of 41 kDa and is 70% similar to 1-propanol dehydrogenase of *E. limosum*, and 41% similar to alcohol dehydrogenase of *C. autoethanogenum* (CAETHG_3279) and ethanol dehydrogenase of *C. ljungdahlii* (CLju_11880). Much to our surprise, deletion of *adh4* stimulated ethanol formation drastically; at the same time, expression of *adh6* was increased. The effect is not easy to explain since Adh4 is

the propanol dehydrogenase involved in 1,2-propanediol metabolism in the BMC. But, in addition to the reduction of propionaldehyde, Adh4 may be also involved in ethanol formation as it has high activity towards reduction of acetaldehyde (Chowdhury *et al*., 2021). The drastic increase in ethanol formation in the Δ*adh4* mutant argues for Adh4 being involved in ethanol utilization. Then, its deletion results in an increase of ethanol. But one could also imagine a regulatory event that apparently led to high *adh6* expression in the Δ*adh4* mutant which led to higher ethanol formation. The role of the *adh* genes can only be addressed in genetic studies using double, triple and multiple mutants since there is, apparently, a high degree of redundancy of the different *adh* genes/proteins. Although our experiments failed to identify the alcohol dehydrogenase catalysing ethanol formation from fructose, the experiments revealed a complex network of enzymes that can substitute for each other. Although *A. woodii* is not known as a natural ethanol producer, our experiments revealed at least the genetic potential of *A. woodii* to produce ethanol.

Taken together, our physiological experiments revealed ethanol production from fructose, as seen before (Buschhorn *et al*., 1989), but not from $H_2 + CO_2$, formate, pyruvate, lactate, or alanine. Previously, ethanol formation was observed at a phosphate concentration between 0.2 and 8.4 mM, with an optimum at 3.2 mM phosphate. Our media had a phosphate concentration of 1.5 mM, not accounting for phosphate in yeast extract. Therefore, our media also allowed for ethanol formation and the effect of phosphate was not further elaborated on. Instead, we concentrated on bicarbonate and Na^+. At low carbon concentration, there was no ethanol formation and ethanol formation was not stimulated by elevated bicarbonate concentrations. At high carbon, ethanol formation increased and was further stimulated by elevated bicarbonate (120 mM). However, the greatest stimulatory effect was by the absence of Na^+. The stimulatory effect of low Na^+ on ethanol formation was confirmed with resting cells. We noticed that ethanol formation correlated with a decrease in pH and indeed, low initial pH values stimulated ethanol formation. Conditions for ethanol formation are comparable to conditions that shift the metabolism from acidogenesis to solventogenesis in *C. acetobutylicum* (Andersch *et al*., 1983; Gottwald and Gottschalk, 1985). The observations are in line with the hypothesis that acetyl-CoA, formed from fructose, is converted to ethanol under high carbon load, to avoid acidification of the medium. Reduced ferredoxin and NADH generated during fructose oxidation are redirected to the reduction of acetyl-CoA. If Na^+ is omitted, electrons cannot flow into the WLP and, again, are redirected to acetyl-CoA. Same is true for low bicarbonate conditions that favour acetyl-CoA reduction but high bicarbonate concentration favours the WLP and thus, electrons flow to the WLP (Fig. 9). Obviously, the model is not compatible with the observed stimulation of ethanol formation by bicarbonate in growing cells. However, stimulation is low compared to low Na^+ conditions and may have to do with an effect of bicarbonate on growth, for carboxylation reactions such as pyruvate carboxylase or phosphoeneolpyruvate carboxylase.

Experimental procedures

Organisms and cultivation

Acetobacterium woodii strains were routinely cultivated under anoxic condition at 30°C either in the complex

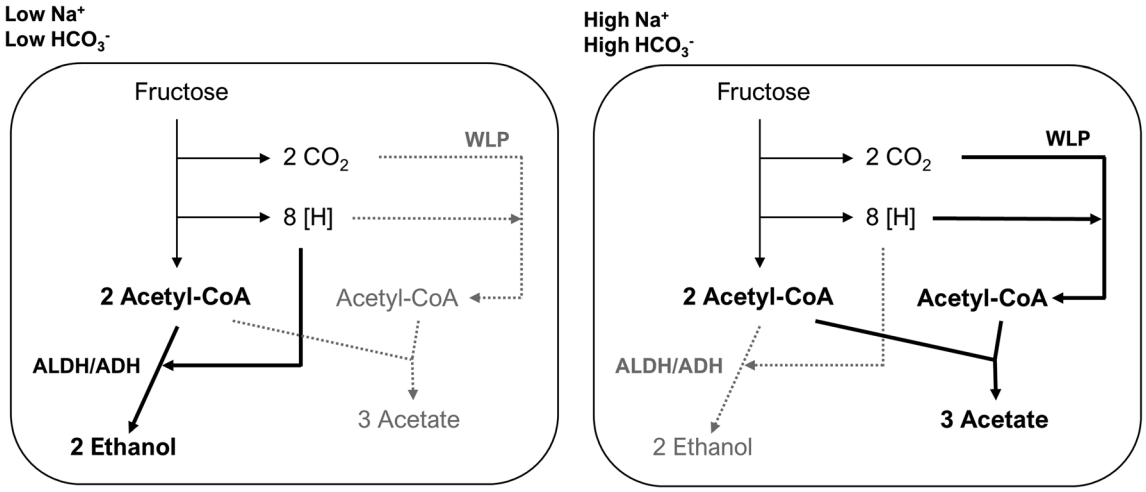

Fig. 9. Electron flow depending on the Na^+ and bicarbonate concentration. Electrons (reduced ferredoxin and NADH) generated during fructose metabolism flow to ethanol formation at low Na^+ or low bicarbonate as the WLP is not favourable (grey lines). On the other hand, at high Na^+ or high bicarbonate electrons flow to the reduction of CO_2 via the WLP to produce one more acetyl-CoA, which leads to homoacetogenesis (black lines).

medium described previously (Heise *et al*., 1989) or Na^+-depleted medium (both media contain 2–3 mM phosphate). The Na^+-depleted medium was prepared identically to carbonated buffered complex medium except that NaCl was substituted by 20 mM KCl. The residual Na^+ concentration was 100 μM. The *A. woodii* strains used in this study are listed in Table S1. As substrates for growth, 20 or 60 mM fructose were used. Growth was monitored by measuring the optical density at 600 nm (OD_{600}).

Preparation of resting cells

Cells of *A. woodii* were grown on 60 mM fructose either in 2 L Na^+-rich (20 mM) or Na^+-depleted complex medium to stationary growth phase (OD_{600} over 2.0) and then harvested by centrifugation (Avanti™J-25 and JA-10 Fixed-Angle Rotor; Beckman Coulter, Brea, CA, USA) at 8000 rpm and 4°C for 10 min. The harvested cells were washed with 30 ml of buffer containing 50 mM imidazole (pH 7.0), 20 mM KCl, 20 mM $MgSO_4$, 4 mM DTE and 4 μM resazurin by centrifugation at 8500 rpm and 4°C for 10 min (AvantiJ-25 and JA-25.50 Fixed-Angle Rotor; Beckman Coulter). Then, the cells were resuspended in 5 ml of buffer in 16 ml Hungate tubes. All steps were performed under strictly oxygen-free conditions in an anoxic chamber (Coy Laboratory Products, Grass Lake, MI, USA) filled with N_2/H_2 (96%–98%/2%–4%; vol./vol.). The total protein concentration in the resting cells was measured using the method of (Schmidt *et al*., 1963).

Cell suspension experiments

Twenty millilitres of buffer (50 mM imidazole, 60 mM $KHCO_3$, 20 mM KCl, 20 mM $MgSO_4$, 4 mM DTE, 4 μM resazurin, pH 7.0) either with 20 mM or without NaCl was used in 115 ml serum flasks under an N_2/CO_2 (80:20, vol.:vol.) atmosphere and cells were added to a total protein concentration of 2 mg ml^{-1}. As substrate, 60 mM fructose was added to the resting cells. The experiments were started by addition of the substrate. One millilitre sample was taken at each time point for determination of metabolites.

Chemical analysis

H_2 was determined by gas chromatography as described previously (Weghoff and Müller, 2016). The concentrations of ethanol and acetate were determined by gas chromatography as described previously (Trifunović *et al*., 2016). The concentrations of fructose, formate and lactate were determined by high-performance liquid chromatography as described previously (Moon *et al*., 2019). Alanine was determined enzymatically using alanine dehydrogenase as described previously (Dönig and Müller, 2018).

Analysis of gene expression levels

Cells of *A. woodii* grown on either 20 or 60 mM fructose in the presence or absence of NaCl were harvested in the exponential or stationary growth phase. Preparation of RNA and cDNA was performed as described previously (Dönig and Müller, 2018). The transcript abundance of the putative *adh* genes was analysed by semiquantitative PCR with 20 cycles as described previously (Bertsch *et al*., 2016). For the expression of *gyrA* and *pduT*, the oligonucleotides GyrA_for_qrtPCR/GyrA_rev_qrtPCR and Awo_c25740 qPCR F/Awo_c25740 qPCR R were used as described previously (Chowdhury *et al*., 2020). The prepared cDNA was used as template and chromosomal DNA of *A. woodii* was used as positive control. The relative expression levels of the *adh3*, *adh4* and *adh6* genes were also analysed with real-time qPCR in a Rotor Gene RG-3000 qPCR cycler (Corbett Research, Cambridge, UK) using iQ SYBR Green Supermix (Bio-Rad Laboratories, Hercules, CA, USA) according to the manufacturer's protocol. The gene *gyrA* (Awo_c00060) was used as housekeeping gene and the relative expression levels were calculated using the $2^{-\Delta\Delta Ct}$ method (Livak and Schmittgen, 2001). For the amplification following oligonucleotides were used: qadh3_for (5′-GTCT TCCGCCATCACTCAC-3′) and qadh3_rev (5′-TTTT CTTTAACAAAGGCCGTATCA-3′) for *adh3*, qadh4_for (5′-GTTATCTGAATGGGTCGGATCTC-3′) and qadh4_rev (5′-CGTGGGCAATACTATGGGTAAT-3′) for *adh4*, and qadh6_for (5′-ATGCAACCGGTATTGGCTTT-3′) and qadh6_rev (5′-TCAATGATTTGGGCATTTTT-3′) for *adh6*.

Generation of A. woodii *Δ*adh3 *and Δ*adh6 *strains*

The plasmids pMTL84151_JM_dadh3 and pMTL84151_JM_dadh6 were constructed in *E. coli* DH5α (New England Biolabs, Frankfurt am Main, Germany) and transformed into *A. woodii* Δ*pyrE* strain, as previously described (Westphal *et al*., 2018). The plasmids were derived from pMTL84151 (Heap *et al*., 2009) but lack a replicon for Gram-positive bacteria. In the plasmids pMTL84151_JM_dadh3 and pMTL84151_JM_dadh6, 1000 bp of UFR and DFR of *adh3* (Awo_c06180) and *adh6* (Awo_c25410) were cloned into the multiple cloning sites. Since these plasmids possess a *catP* marker for chloramphenicol/thiamphenicol resistance from *C. perfringens* (Werner *et al*., 1977) and the *pyrE* from *C. acetobutylicum* (Westphal *et al*., 2018) as a counter selectable marker, the first selection was achieved in an agar plate with complex medium supplemented with

20 mM fructose and 30 ng μl^{-1} thiamphenicol after transformation of plasmids into *A. woodii* Δ*pyrE* strain by electroporation (625 V, 25 μF, 600 Ω, in 1 mm cuvettes). Then, the thiamphenicol-resistant colonies were further plated onto an agar plate with minimal medium (Westphal *et al*., 2018) supplemented with 20 mM fructose, 1 μg ml^{-1} uracil and 1 mg ml^{-1} 5-FOA for disintegration. The deleted region was analysed by PCR with oligonucleotides which bind in front of UFR and behind DFR of the respective gene: aus_adh3_for (5′-ACAGTAGCTGGAAATGTGATTAG-3′) and aus_adh3_rev (5′-CGTATCATGACCCTTAAACTATTTTGC-3′) for Δ*adh3*, and aus_adh6_for (5′-CCAGATGCATTGACCTTTTCTA-3′) and aus_adh6_rev (5′-TTGTTATGCGGGTTATTTTTGGC-3′) for Δ*adh6* respectively. The deleted regions of the mutants were verified by Sanger sequencing as well (Sanger *et al*., 1977).

Acknowledgements

We are indebted to the European Research Council (ERC) for financial support under the European Union's Horizon 2020 research and innovation program (ACETOGENS, Grant Agreement No. 741791).

References

Andersch, W., Bahl, H., and Gottschalk, G. (1983) Level of enzymes involved in acetate, butyrate, acetone and butanol formation by *Clostridium acetobutylicum*. *Eur J Appl Microbiol Biotechnol* **18**: 327–332.

Basen, M., Schut, G.J., Nguyen, D.M., Lipscomb, G.L., Benn, R.A., Prybol, C.J., *et al*. (2014) Single gene insertion drives bioalcohol production by a thermophilic archaeon. *Proc Natl Acad Sci U S A* **111**: 17618–17623.

Bertsch, J., and Müller, V. (2015) Bioenergetic constraints for conversion of syngas to biofuels in acetogenic bacteria. *Biotechnol Biofuels* **8**: 210.

Bertsch, J., Siemund, A.L., Kremp, F., and Müller, V. (2016) A novel route for ethanol oxidation in the acetogenic bacterium *Acetobacterium woodii*: the acetaldehyde/ethanol dehydrogenase pathway. *Environ Microbiol* **18**: 2913–2922.

Boiteux, A., and Hess, B. (1970) Allosteric properties of yeast pyruvate decarboxylase. *FEBS Lett* **9**: 293–296.

Buschhorn, H. (1989) *Physiologische, enzymatische und genetische Untersuchungen zum Ethanol-Stoffwechsel von* Acetobacterium woodii. Göttingen: Georg-August-Universität zu Göttingen.

Buschhorn, H., Dürre, P., and Gottschalk, G. (1989) Production and utilization of ethanol by the homoacetogen *Acetobacterium woodii*. *Appl Environ Microbiol* **55**: 1835–1840.

Buschhorn, H., Dürre, P., and Gottschalk, G. (1992) Purification and properties of the coenzyme A-linked acetaldehyde dehydrogenase of *Acetobacterium woodii*. *Arch Microbiol* **158**: 132–138.

Chowdhury, N.P., Alberti, L., Linder, M., and Müller, V. (2020) Exploring bacterial microcompartments in the acetogenic bacterium *Acetobacterium woodii*. *Front Microbiol* **11**: 593467.

Chowdhury, N.P., Moon, J., and Müller, V. (2021) Adh4, an alcohol dehydrogenase controls alcohol formation within bacterial microcompartments in the acetogenic bacterium *Acetobacterium woodii*. *Environ Microbiol* **23**: 499–511.

Daniell, J., Köpke, M., and Simpson, S.D. (2012) Commercial biomass syngas fermentation. *Energies* **5**: 5372–5417.

Dien, B.S., Cotta, M.A., and Jeffries, T.W. (2003) Bacteria engineered for fuel ethanol production: current status. *Appl Microbiol Biotechnol* **63**: 258–266.

Dönig, J., and Müller, V. (2018) Alanine, a novel growth substrate for the acetogenic bacterium *Acetobacterium woodii*. *Appl Environ Microbiol* **84**: e02023-18.

Fawzy, S., Osman, A.I., Doran, J., and Rooney, D.W. (2020) Strategies for mitigation of climate change: a review. *Environ Chem Lett* **18**: 2069–2094.

Gabrielli, P., Gazzani, M., and Mazzotti, M. (2020) The role of carbon capture and utilization, carbon capture and storage, and biomass to enable a net-zero-CO_2 emissions chemical industry. *Ind Eng Chem Res* **59**: 7033–7045.

Gottwald, M., and Gottschalk, G. (1985) The internal pH of *Clostridium acetobutylicum* and its effect on the shift from acid to solvent formation. *Arch Microbiol* **143**: 42–46.

Heap, J.T., Pennington, O.J., Cartman, S.T., and Minton, N. P. (2009) A modular system for *Clostridium* shuttle plasmids. *J Microbiol Methods* **78**: 79–85.

Heise, R., Müller, V., and Gottschalk, G. (1989) Sodium dependence of acetate formation by the acetogenic bacterium *Acetobacterium woodii*. *J Bacteriol* **171**: 5473–5478.

Liew, F., Henstra, A.M., Köpke, M., Winzer, K., Simpson, S. D., and Minton, N.P. (2017) Metabolic engineering of *Clostridium autoethanogenum* for selective alcohol production. *Metab Eng* **40**: 104–114.

Liew, F., Henstra, A.M., Winzer, K., Köpke, M., Simpson, S. D., and Minton, N.P. (2016a) Insights into CO_2 fixation pathway of *Clostridium autoethanogenum* by targeted mutagenesis. *mBio* **7**: e00427-16.

Liew, F., Martin, M.E., Tappel, R.C., Heijstra, B.D., Mihalcea, C., and Köpke, M. (2016b) Gas fermentation-a flexible platform for commercial scale production of low-carbon-fuels and chemicals from waste and renewable feedstocks. *Front Microbiol* **7**: 694.

Livak, K.J., and Schmittgen, T.D. (2001) Analysis of relative gene expression data using real-time quantitative PCR and the $2^{-\Delta\Delta Ct}$ method. *Methods* **25**: 402–408.

Ljungdahl, L.G. (1986) The autotrophic pathway of acetate synthesis in acetogenic bacteria. *Ann Rev Microbiol* **40**: 415–450.

Membrillo-Hernandez, J., and Lin, E.C. (1999) Regulation of expression of the *adhE* gene, encoding ethanol oxidoreductase in *Escherichia coli*: transcription from a downstream promoter and regulation by Fnr and RpoS. *J Bacteriol* **181**: 7571–7579.

Moon, J., Henke, L., Merz, N., and Basen, M. (2019) A thermostable mannitol-1-phosphate dehydrogenase is required in mannitol metabolism of the thermophilic acetogenic bacterium *Thermoanaerobacter kivui*. *Environ Microbiol* **21**: 3728–3736.

Müller, V. (2003) Energy conservation in acetogenic bacteria. *Appl Environ Microbiol* **69**: 6345–6353.

Müller, V. (2014) Bioalcohol production by a new synthetic route in a hyperthermophilic archaeon. *Proc Natl Acad Sci U S A* **111**: 17352–17353.

Müller, V. (2019) New horizons in acetogenic conversion of one-carbon substrates and biological hydrogen storage. *Trends Biotechnol* **37**: 1344–1354.

Müller, V., Blaut, M., Heise, R., Winner, C., and Gottschalk, G. (1990) Sodium bioenergetics in methanogens and acetogens. *FEMS Microbiol Rev* **87**: 373–377.

Nissen, L.S., and Basen, M. (2019) The emerging role of aldehyde:ferredoxin oxidoreductases in microbially-catalyzed alcohol production. *J Biotechnol* **306**: 105–117.

Poehlein, A., Schmidt, S., Kaster, A.-K., Goenrich, M., Vollmers, J., Thürmer, A., *et al*. (2012) An ancient pathway combining carbon dioxide fixation with the generation and utilization of a sodium ion gradient for ATP synthesis. *PLoS One* **7**: e33439.

Richter, H., Molitor, B., Diender, M., Sousa, D.Z., and Angenent, L.T. (2016a) A narrow pH range supports butanol, hexanol, and octanol production from syngas in a continuous co-culture of *Clostridium ljungdahlii* and *Clostridium kluyveri* with in-line product extraction. *Front Microbiol* **7**: 1773.

Richter, H., Molitor, B., Wei, H., Chen, W., Aristilde, L., and Angenent, L.T. (2016b) Ethanol production in syngas-fermenting *Clostridium ljungdahlii* is controlled by thermodynamics rather than by enzyme expression. *Energ Environ Sci* **9**: 2392–2399.

Sanger, F.S., Nickelen, F., and Coulson, A.R. (1977) DNA-sequencing with chain-terminating inhibitors. *Proc Natl Acad Sci U S A* **74**: 5463–5467.

Schmidt, K., Liaaen-Jensen, S., and Schlegel, H.G. (1963) Die Carotinoide der *Thiorhodaceae*. *Arch Mikrobiol* **46**: 117–126.

Schuchmann, K., and Müller, V. (2014) Autotrophy at the thermodynamic limit of life: a model for energy conservation in acetogenic bacteria. *Nat Rev Microbiol* **12**: 809–821.

Schuchmann, K., Schmidt, S., Martinez Lopez, A., Kaberline, C., Kuhns, M., Lorenzen, W., *et al*. (2015) Nonacetogenic growth of the acetogen *Acetobacterium woodii* on 1,2-propanediol. *J Bacteriol* **197**: 382–391.

Trifunović, D., Schuchmann, K., and Müller, V. (2016) Ethylene glycol metabolism in the acetogen *Acetobacterium woodii*. *J Bacteriol* **198**: 1058–1065.

Weghoff, M.C., and Müller, V. (2016) CO metabolism in the thermophilic acetogen *Thermoanaerobacter kivui*. *Appl Environ Microbiol* **82**: 2312–2319.

Werner, H., Krasemann, C., Gorniak, W., Hermann, A., and Ungerechts, J. (1977) Die Thiamphenicol- und Chloramphenicol-Empfindlichkeit von Anaerobiern. *Zentralbl Bakteriol Orig A* **237**: 358–371.

Westphal, L., Wiechmann, A., Baker, J., Minton, N.P., and Müller, V. (2018) The Rnf complex is an energy coupled transhydrogenase essential to reversibly link cellular NADH and ferredoxin pools in the acetogen *Acetobacterium woodii*. *J Bacteriol* **200**: e00357-18.

White, H., Huber, C., Feicht, R., and Simon, H. (1993) On a reversible molybdenum-containing aldehyde oxidoreductase from *Clostridium formicoaceticum*. *Arch Microbiol* **159**: 244–249.

Wood, H.G., and Ljungdahl, L.G. (1991) Autotrophic character of the acetogenic bacteria. In *Variations in Autotrophic Life*, Shively, J.M., and Barton, L.L. (eds). San Diego: Academic Press, pp. 201–250.

Supporting Information

Additional Supporting Information may be found in the online version of this article at the publisher's web-site:

Table S1. *A. woodii* strains used in this study.

Fig. S1. Conversion of fructose into acetate and ethanol by resting cells of *A. woodii* in dependence of the initial pH of the buffer. During the cell suspension experiments presented in Fig. 4, fructose (A), acetate (B), and ethanol (C) were determined in cell suspensions incubated in buffer with an initial pH of 7.4 (■), 6.9 (▲), 6.6 (•), or 6.2 (◆). Each data point indicates a mean ± SEM; n = 2 independent experiments.

Fig. S2. Transcript abundance of genes encoding putative alcohol dehydrogenases in *A. woodii.* Cells were grown in Na^{+-} depleted or Na^{+-} rich (20 mM) complex media with either 20 or 60 mM fructose. At exponential or stationary growth phase, cells were harvested for mRNA preparation and cDNA synthesis. The transcript levels of the 11 putative *adh* genes were analyzed with semi-quantitative PCR with 80 ng of cDNA as template using 20 cycles. The expression of a house keeping gene *gyrA* and the highly expressed gene *pduT* was also analyzed for checking quality of cDNA. Chromosomal DNA (gDNA) of *A. woodii* was used as positive control. No template was used for the last lane (_) as negative control. The data shown are representative for two independent experiments.

Fig. S3. Genotypic analysis of *A. woodii* Δ*adh3* and Δ*adh6* using colony PCR. DNA fragments of deleted regions from the mutants were analyzed on a 1.0% agarose gel. DNA fragment for Δ*adh3*; 3386 bp by the wild type and 2156 bp by Δ*adh3*. DNA fragment for Δ*adh6*; 3303 bp by the wild type and 2160 bp by Δ*adh6*. The primers used for verification are described in Experimental procedures.